Electronic Supplementary Material (ESI) for Environmental Science: Nano.

A novel covalent organic framework for efficient photocatalytic reduction of Cr (VI) and synergistic removal of organic pollutants under visible light irradiation

Supporting Information

1. Characterizations

The crystal structure of HDU-26 was analyzed by X-ray diffraction (XRD, SmartLab SE). The morphology of HDU-26 was determined by transmission electron microscopy (TEM, FEI Tecnai F20) and scanning electron microscopy (SEM, ZEISS Gemini 300). Brunauer−Emmett−Teller (BET) measurements were conducted using N_2 adsorption/desorption technique (TriStar II 3020). Thermogravimetric analysis (TG, STA 2500) of HDU-26 was carried out at a heating rate of 10 °C min^{-1} in nitrogen under stable reaction conditions from 25 to 800 °C. The Fourier-transform infrared (FTIR) transmission spectra are measured on a SHIMADZU-IRT racer-100 spectrometric analyzer. The elemental composition and chemical state of the samples were analyzed using an X-ray photoelectron spectroscopy (XPS, Thermo Scientific ESCALAB 250Xi). Solid-state ^{13}C nuclear magnetic resonance (NMR, Bruker 400 MHz) spectroscopy further determined the chemical structure of HDU-26. The diffuse reflectance spectra (DRS) were collected using a Shimadzu UV-2700 UV–vis spectrophotometer ($BaSO_4$ as a reflectance standard). The zeta potentials at different pH values were determined by a Zetasizer Nano ZSE. All the electrochemical characterizations were performed on a CHI 760D electrochemical analyzer (Chenhua,

Shanghai, China) in a standard three-electrode system, where the Ag/AgCl electrode is the counter electrode and the Pt sheet is the counter electrode. The photocatalytic chamber (CEL-LB70) and the xenon light source system (CEL-HXF300-T3) were provided by CEAULIGHT.

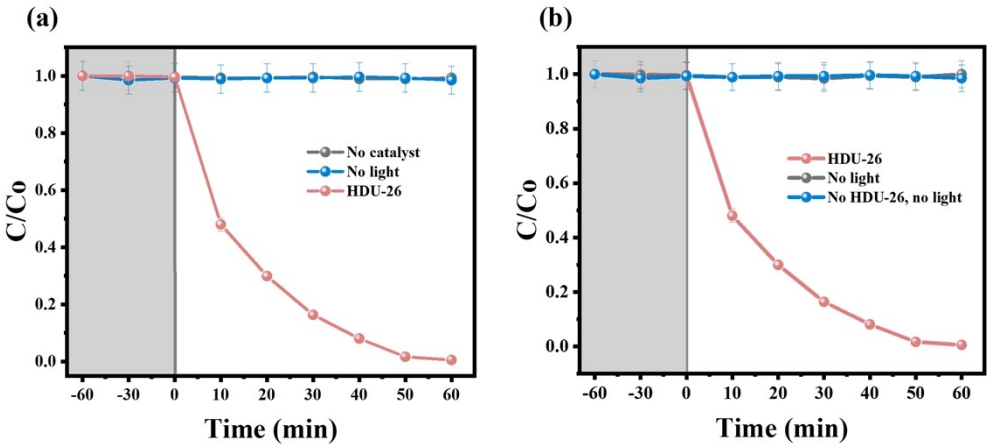

Fig. S1. (a) Degradation efficiency of Cr(VI) in different systems. (b) Comparison between with and without the HDU-26 catalyst under dark conditions.

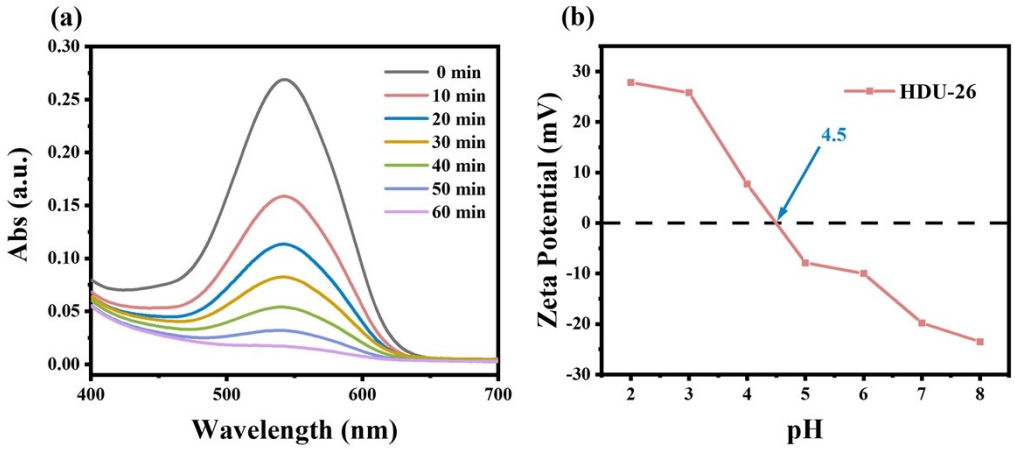

Fig. S2. (a) UV−vis absorption curves of photocatalytic reduction of Cr(VI) at different times. (b) Zeta potential of HDU-26 under different pH values.

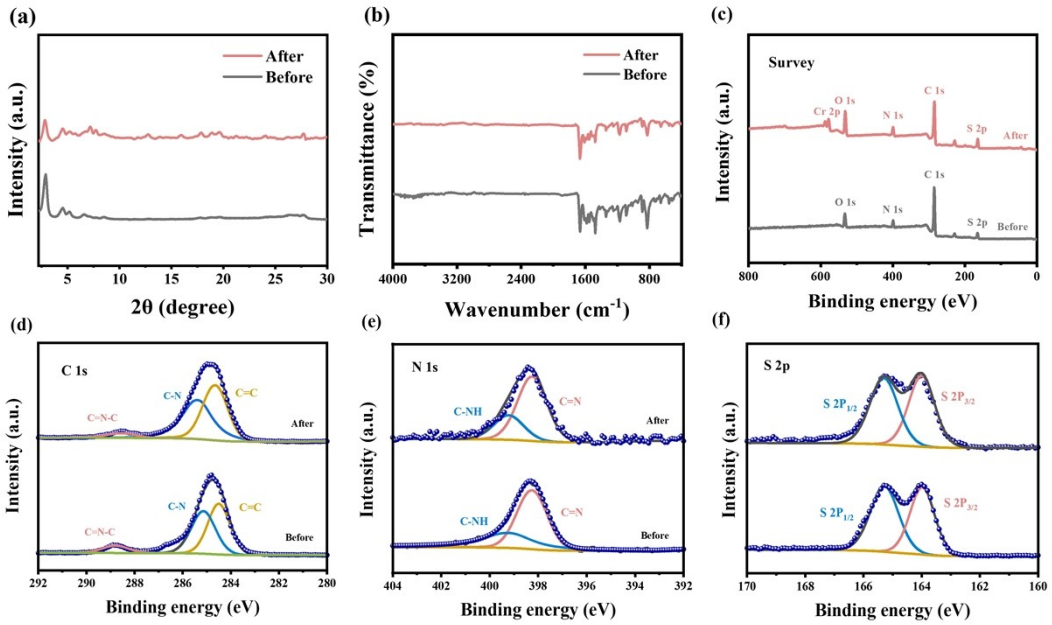

Fig. S3. XRD patterns and FT-IR spectra of HDU-26 before and after photocatalytic reduction of Cr (VI) (a and b). Survey and element XPS spectra of HDU-26 before and

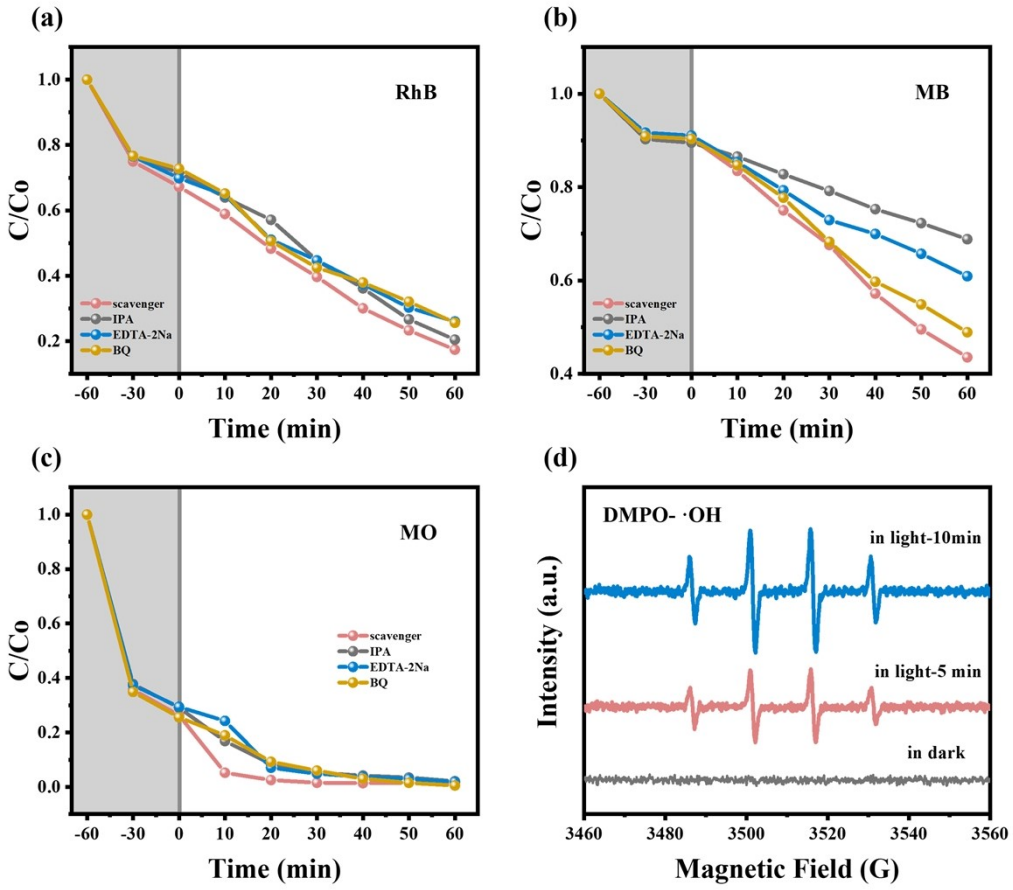

after photocatalytic reduction of Cr (VI) (c-f).

Fig. S4. Effect of different free radical scavengers on photocatalytic degradation of (a) RhB. (b) MB. (c) MO. (d) ESR spectrum by DMPO spin-trapping for ·OH.